Korean J. Chem. Eng., 36(4), 591-599 (2019)
DOI: 10.1007/s11814-018-0201-y

pISSN: 0256-1115
eISSN: 1975-7220

Photo-crosslinked polymer networks based on graphene-functionalized soybean oil and their properties

Hui Wang, Arvind Gupta, and Beom Soo Kim†

Department of Chemical Engineering, Chungbuk National University, Cheongju, Chungbuk 28644, Korea
(*Received 2 September 2018 • accepted 26 November 2018*)

Abstract−The increasing importance of products which are sustainable and eco-friendly drives the scientific community to develop materials derived from bio-based and agricultural feedstock. With the same motivation, we have developed acrylated epoxidized soybean oil (AESO)-based composite with functionalized graphene or graphene oxide using UV curing technique. Graphene and graphene oxide were chemically functionalized with 3-methacryloxypropyltrimethoxysilane and 4,4′-diphenylmethanediisocyanate/hydroxyl ethyl acrylate, respectively, and used as filler in the AESO matrix. Infra-red and X-ray photoelectron spectroscopy confirmed the functionalization of graphene and graphene oxide along with formation of polymer network in composite. Functionalization of graphene and graphene oxide was found to be effective in enhancing homogeneous dispersion into the polymer matrix, which ultimately improved mechanical properties of base polymer (~48% increase in tensile strength with 0.02% addition of functionalized graphene). On the other hand, AESO composite with graphene and graphene oxide without functionalization exhibited lower tensile strengths. The functionalization of graphene and graphene oxide and incorporation of the same in the polymer network using UV curing technique provides a realistic and effective methodology to obtain high performance composite for several applications.

Keywords: Acrylated Epoxidized Soybean Oil, Functionalized Graphene, Nanocomposites, UV Curing

INTRODUCTION

As the importance of sustainable and environmentally friendly products increases to reduce dependence on petroleum, the scientific community is developing materials derived from bio-based and agricultural feedstocks [1]. Several bio-based polymers and polymerizable substances have received significant attention over the past few decades. As a renewable resource, triglyceride plant oils such as soybean oil have been utilized in the production of polymeric materials. Soybean oil is potentially biodegradable, low in toxicity, biocompatible, relatively cheap, and abundantly available worldwide. Soybean oil contains double bond in its chemical structure which can be epoxidized and reacted with acrylic acid resulting in acrylated epoxidized soybean oil (AESO) [2,3]. Biomedical, cosmetics, food industry, alternative fuels, agrochemicals, and polymer industries are the broad areas where AESO is being utilized. AESO has been used extensively in the production of polymers and copolymers for a variety of applications [4,5]. Due to the inherent limitations of relatively poor mechanical strength, the use of AESO is hindered in several areas such as engineering applications [6].

Numerous techniques have been developed to improve the properties of AESO-based polymers such as copolymers [7], bio-composite development [8], and crosslinking with other polymers [9]. The development of bio-composites with different fillers such as natural fibers [10], lignin [11], and carbon materials [12-14] has been found to be an effective formulation for improving the properties of AESO-based polymers. For instance, microcrystalline cellulose (MCC) was incorporated in AESO as a nanofiller [15]. Carbon materials such as graphene, graphene oxide, carbon nanotube, and carbon black are potential fillers for the development of bio-composites.

Graphene, a two-dimensional layer of carbon atoms, has fascinated the scientific community [16-18]. Due to its several unique properties, it has been used as a filler for the fabrication of composites to improve the properties of polymers [19-21]. Although addition of graphene or graphene oxide into various polymer matrices has remarkably improved polymer properties, homogeneous dispersion of graphene still requires detailed investigations [22-24]. It has been found that graphene and graphene oxide are not homogeneously dispersed into the polymer matrix due to the π-π interaction and stacking by van der Waals interaction between graphene or graphene oxide sheets [25]. Additionally, a strong bond between the filler and the matrix is essential to obtain improved properties, which is a major challenge [24]. There is a sufficient amount of literature to improve the dispersion of graphene into the polymer matrix [26-30]. Chemical modification of graphene and graphene oxide has been found to be an effective approach due to the presence of epoxy and hydroxyl functional groups on the molecular surface for modification [31-36]. Achieving highly dispersed graphene in polymer matrices often requires mechanical techniques and complex surface chemistry such as covalent functionalization of graphene by ester linkages [37] and amide linkages [36,38]. The modification of graphene using chemical functionalization significantly weakens intermolecular interactions and prevents agglomeration.

†To whom correspondence should be addressed.
E-mail: bskim@chungbuk.ac.kr

To achieve good dispersion of graphene, Wang et al. [39] functionalized graphene using 3-methacryloxypropyltrimethoxysilane and covalently incorporated it into polyurethane acrylate matrix using UV curing technology and found 16 °C increase in the thermal degradation temperature. Similarly, Yu et al. [40] functionalized graphene oxide with acrylate active end-group followed by covalently reinforcing into acrylated polyurethane using UV curing technique. Improved interfacial interaction between functionalized graphene and polymer matrix was observed.

In this study, four types of soybean oil/graphene-based photocrosslinked polymer networks, AESO/graphene, AESO/graphene oxide, AESO/functionalized graphene, and AESO/functionalized graphene oxide, were prepared and characterized. Graphene was produced by exfoliation of graphite using plant extract [41,42]. Functionalized graphene and graphene oxide were prepared by introducing acrylate functionalities into the graphene and graphene oxide using the reported procedures [39,40]. The effect of functionalization on the properties of composite was investigated and compared with graphene and graphene oxide without functionalization.

MATERIALS AND METHODS

1. Materials

Graphene oxide (GO) was procured from Standard Graphene Corp. (Korea) and expanded graphite was purchased from Samjung C&G (Korea). Acrylated epoxidized soybean oil (AESO), 3-methacryloxypropyltrimethoxysilane (MPTMS), hydroxylethylacrylate (HEA), 4,4′-diphenylmethanediisocyanate (MDI), hydrazine hydrate (80%), 4-methoxyphenol, and 2,2-dimethoxy-2-phenylacetophenone (DMPA) were purchased from Sigma-Aldrich (USA). Hydrochloric acid, chloroform, and acetone were obtained from Samchun Chemicals (Korea). N,N-dimethylformamide (DMF) was obtained from Tedia Company Inc. (USA). All chemicals were used as received without further purification and were of analytical grade unless otherwise specified.

2. Preparation of Plant Extract

Plant extract was prepared using the procedure obtained elsewhere [41], wherein 5 g of *Xanthium strumarium* was added to 300 mL Erlenmeyer flask to which 100 mL of sterile distilled water was added. The mixture was heated to 100 °C and allowed to boil for 15 min. After heating, the plant extract was dissolved into the water which was decanted and stored at 4 °C and used within a week.

3. Preparation of Graphene

Procedure for preparing graphene (GN) using plant extract was adopted from elsewhere [42]. Briefly, 0.2 g of expanded graphite was dispersed into 180 mL deionized water. 20 mL plant extract (50 g/L) was added to the water/graphite dispersion. Low power sonication approach was adopted to maintain the temperature at 60 °C with continuous flow of water in a sonication bath. Sonication was done for 24 h followed by centrifugation at 250 g for 45 min. The stably dispersed supernatant was collected and freeze dried at −50 °C for 24 h and used for further study.

4. Preparation of Functionalized Graphene

Functionalized graphene (FGN) was prepared using the procedure described by Wang et al. [39]. Briefly, GO is recognized as a carbon monolayer with randomly distributed sp^2 and sp^3 carbon atoms containing epoxy, carboxyl, carbonyl, and hydroxyl functional groups [43]. Presence of these functional groups could act as active sites to react with MPTMS (Scheme 1). 50 mg of GO was dispersed in 10 mL of MPTMS along with 2 mL of HCl and diluted with 250 mL of deionized water in a round bottomed flask. The flask was kept in an ultrasonication bath for 1 h in order to make a stable dispersion. Temperature of the flask was increased to 75 °C for the hydrolysis of MPTMS and condensation of GO for 2 h. Addition of 1.5 mL of hydrazine solution to the suspension reduced GO, which resulted in FGN. The final solution was filtered and washed using deionized water repeatedly to get pH near 7 followed by freeze drying at −50 °C under reduced pressure for 24 h.

5. Preparation of Functionalized Graphene Oxide

Functionalized graphene oxide (FGO) was prepared as men-

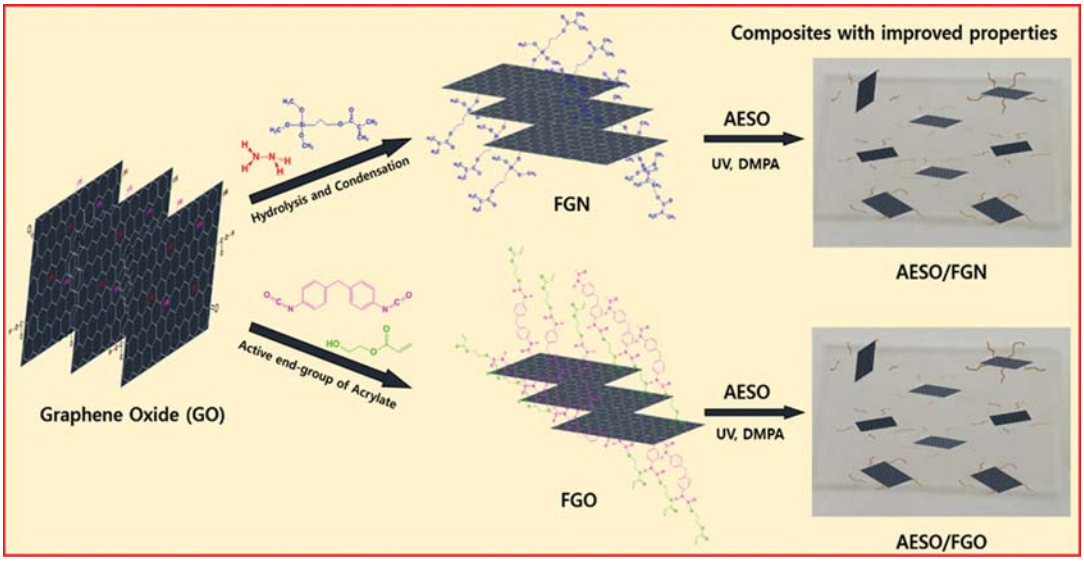

Scheme 1. Schematic diagram for functionalization routes of GO and composite preparation.

tioned in the literature [40]. For this, 600 mg of GO was added in a flask containing 60 mL of DMF and kept in an ultrasonication bath for 30 min for homogeneous dispersion. The suspension was transferred into a 250 mL four-necked flask connected with nitrogen inlet, dropping funnel, reflux condenser, and mechanical stirrer. The flask was flushed with nitrogen gas to remove any oxygen and moisture molecules present in the flask, and temperature was increased to 70 °C. Thereafter, 14.28 g of MDI (solution in 10 mL of DMF) was added dropwise using a dropping funnel and left for 3 h. The reaction mixture obtained was cooled to 50 °C, and 0.1 g of 4-methoxyphenol and 14.3 g of HEA were added and stirred for 12 h. The resulting suspension was subjected to filtration unit followed by washing using chloroform. The washed content was collected as FGO and freeze dried at −50 °C under reduced pressure. Schematic diagram for functionalization is shown in Scheme 1.

6. Preparation of Cross-linked Polymer

All UV-cured cross-linked polymer composites were prepared using solution casting technique [44]. Predetermined amount of GO, FGO, GN, or FGN powders was dispersed in a fixed volume of DMF by sonication at room temperature. The fixed amount of AESO was subsequently introduced into the dispersion and stirred for 1 h. The cross-linking occurred by radical-initiated UV photopolymerization after addition of 2 wt% initiator (0.1 g of DMPA in 1 mL of 1-vinylpyrrolidinone). The composite samples were developed as thin films of approximately 100 μm where 0.5 mL of the reaction mixture was employed between two glass plates (150 mm× 150 mm) and kept for polymerization under UV lamp (1.2 kW) at 366 nm for 15 min in air at room temperature. A series of UV-cured AESO/GO (0%, 0.02%, 0.05%, 0.10%, 0.15%, 0.20%, 0.25%), AESO/FGO (0%, 0.02%, 0.05%, 0.10%, 0.15%, 0.20%, 0.25%), AESO/GN (0%, 0.02%, 0.05%, 0.10%, 0.15%), and AESO/FGN (0%, 0.02%, 0.05%, 0.10%, 0.15%) cross-linked films were formed and named as AESO/GO-X, AESO/FGO-X, AESO/GN-X, and AESO/FGN-X, respectively, where X is the percentage content of filler.

7. Characterization

Fourier transform infrared (FTIR) spectra of the specimens was obtained by transmittance mode in Nicolet IR 200 (Thermo, USA) instrument in the range between wavenumber 4,000 cm^{-1} and 750 cm^{-1}. The pellets for characterization were prepared by mixing samples with potassium bromide (KBr), followed by hydraulic press, and the spectra were recorded against KBr as blank reference.

Thermal transitions of prepared composites were analyzed using differential scanning calorimetry (DSC) (TA Instruments, DSC Q2000). Samples (1-2 mg) were heated from 5 °C to 190 °C at constant rate of 10 °C/min in nitrogen environment.

X-ray photoelectron spectroscopy (XPS) was used to analyze elements and their state in the samples. The powder samples were measured using an XPS system (PHI Quantera-II, Ulvac-PHI) with a monochromatized Al Kα radiation X-ray at 1,486.6 eV and 20 kV argon gas cluster ion beam gun (VG Science, ESCALAB 210, UK). Deconvolution of the XPS spectra was done by assuming that the peaks were Gaussian.

Gel content was measured after 24 h of extraction in chloroform in order to understand the fraction of cross-linked network in the samples. After polymerization, the samples were dried under reduced pressure for 24 h. The films were weighed (W_1) before extraction, and the finally vacuum dried sample after extraction with chloroform weighed as W_2. The gel content was calculated using Eq. (1).

$$\text{Gel content (\%)} = \frac{W_2}{W_1} \times 100 \quad (1)$$

The tensile strength and percentage elongation at break of the cross-linked films were evaluated as per ASTM D-882 standard using

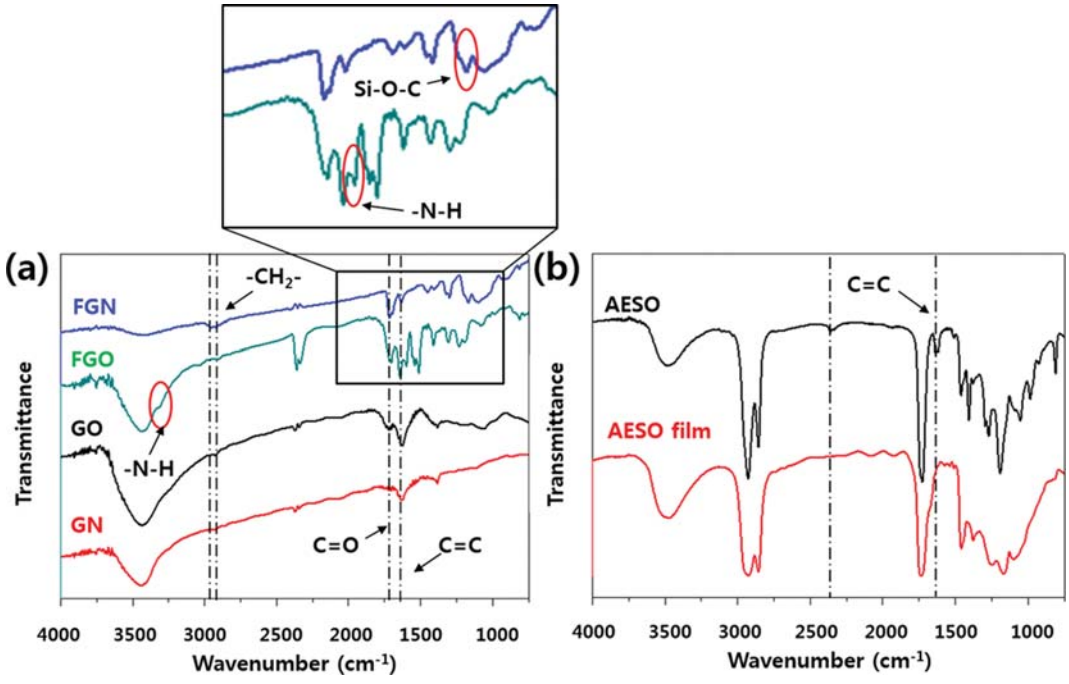

Fig. 1. FTIR spectra of (a) GO, GN, FGO, FGN, (b) AESO and AESO film.

a universal testing machine (UTM) (LR-30K, LLOYD Instruments). The analysis was conducted using 1 kN load cell with cross head speed of 5 mm/min in tensile mode. The dimensions of each specimen were kept as 15 mm×5 mm×0.1 mm (length×width×thickness). An average value of at least eight tested specimens was reported with standard error bar.

The fractured surfaces of the cross-linked films after tensile test were examined using field emission scanning electron microscopy (FE-SEM, LEO-1530, Carl Zeiss). Before analysis, the specimens were gold coated using sputtering technique. The transparency of the cross-linked films was evaluated by UV-Vis spectrophotometer (UV mini-1240, Shimadzu, Japan). The analysis was recorded in the transmission mode in the wavelength range from 200 to 800 nm with air as reference.

RESULTS AND DISCUSSION

1. Structural and Morphological Analysis

FTIR is a powerful tool for the molecular structural analysis of compounds. The FTIR spectra of GO, GN, FGO, FGN, AESO, and cured AESO film are shown in Fig. 1. As shown in Fig. 1(a), the band representing graphene oxide is available at characteristic absorption peaks, i.e., 3,379 cm^{-1}, 1,724 cm^{-1}, 1,623 cm^{-1}, 1,226 cm^{-1}, and 1,043 cm^{-1} corresponding to -OH, C=O carboxyl stretching vibration, C=C in aromatic ring, -COO-, and C-O-C in epoxide, respectively, which are in agreement with available literature [45]. In case of FGO, new absorption peaks are found at around 2,924 and 2,854 cm^{-1}, which are attributed to the symmetric and asymmetric vibration of -CH_2- groups after the GO functionalization with HEA and MDI. Moreover, the stretching vibrations of -NH- groups at 3,393 cm^{-1} together with the carbonyl bands at 1,705 cm^{-1} are found to appear due to the urethane bond formation. The characteristic peaks at 1,635 cm^{-1} and 811 cm^{-1} correspond to the C=C vibration, while the band at 1,412 cm^{-1} is allocated to the bending vibration of C-H, representing the chemical bonding of HEA on the molecular surface of graphene oxide layer through the reaction between hydroxyl and carboxylic groups with isocyanate groups. The disappearance of the peak of the isocyanate group of MDI at 2,264 cm^{-1} also confirms the chemical reaction. The stretching vibration of acrylate attached with the surface of graphene sheet can be confirmed by the increased intensity of C=O stretching band of FGN and peak at 1,633 cm^{-1} can be assigned to C=C group in MPTMS. Due to the presence of Si-O-C or Si-O-Si vibration mode, a new band appears at around 1,100 cm^{-1}. In the spectra of AESO, characteristic peaks are found at 3,400 cm^{-1} (-OH), 2,930 cm^{-1}, 2,850 cm^{-1} (-CH_2-), 1,750 cm^{-1} (C=O), and 1,633 cm^{-1} (C=C), respectively. Furthermore, the disappearance of peaks related to C=C bond (Fig. 1(b)) suggests that these unsaturated bonds present in AESO, FGO, and FGN were polymerized during the curing procedure.

Thermal transitions of the prepared composites (0.02% filler content) were analyzed using DSC (Fig. 2). It was found that developed crosslink network in composites hinder the polymer chains to form crystallites and show no crystallization and melting enthalpy in thermogram. The glass transition temperature of AESO was found to be 33.5 °C, which was enhanced to 42.3 °C due to the addition of the fillers. Glass transition was slightly improved due to functionalization of the fillers, which suggests that presence of fillers and its functionalization obstruct the polymer chains, requiring more energy for vibration.

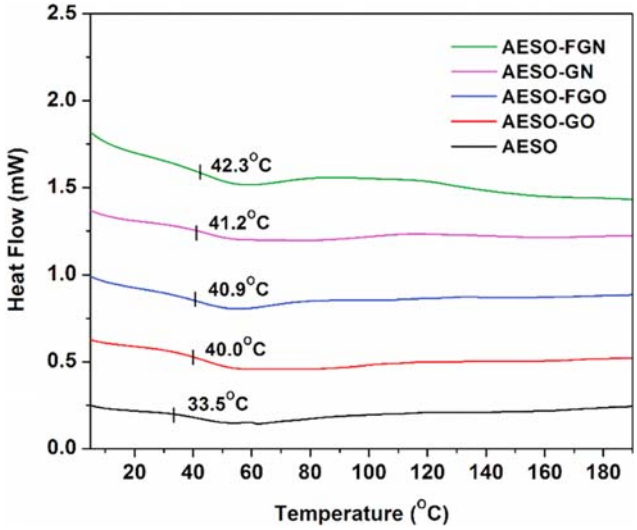

Fig. 2. Representative thermogram of the AESO and prepared composites (0.02% filler addition).

X-ray photoelectron spectroscopy was employed to further confirm the structure of GO, GN, FGO, and FGN and also evaluate composition before and after functionalization. The analysis, C_{1s} XPS spectra of GO, GN, FGO, and FGN and XPS spectra of GO, GN, FGO, and FGN are shown in Fig. 3. The C_{1s} XPS spectrum of fillers can be deconvoluted into four peaks resultant to carbon atoms in different functional groups. The characteristic peaks at 284.4, 286.5, 287.7, and 288.7 eV correspond to unoxidized carbon (C-C), the C atoms in graphite hydroxyl and epoxy/ether groups (C-O), carboxyl groups (C=O), and carboxylate groups (O-C=O), respectively [46]. The C_{1s} XPS spectrum of GN, FGO, and FGN (Fig. 3(b), 3(c), 3(d)) also exhibits carbon functionality as graphite. The peak intensity of oxygenated C in the epoxy/ether groups in GN, FGO, and FGN is relatively lower than that in GO. Whereas, the intensity of oxygenated C in C=O groups is comparatively strong, which originates due to the reaction of acrylate group in MPTMS on FGN and in MDI/HEA on FGO. In Fig. 3(e), the XPS spectrum of FGN shows a signal for the Si_{2p} peak and Si_{2s} peak, which represent the presence of silane group in the system, whereas FGO shows N_{1s} peak corresponding to the isocyanate group in the macromolecules. The presence of peaks related to Si and N suggests the covalent functionalization of graphene.

Gel content analysis of the composites was done to examine polymer network formation. The gel content of AESO film and its composite films are condensed in Table 1. The gel content of all samples was higher than 97%, which indicates that a highly cross-linked polymer network was formed in the composite after UV curing treatment. This also suggests that 97% of the ingredients used was consumed for the formation of polymer network.

2. Mechanical Property

The effect of fillers with and without functionalization on the mechanical property of composites was examined using UTM

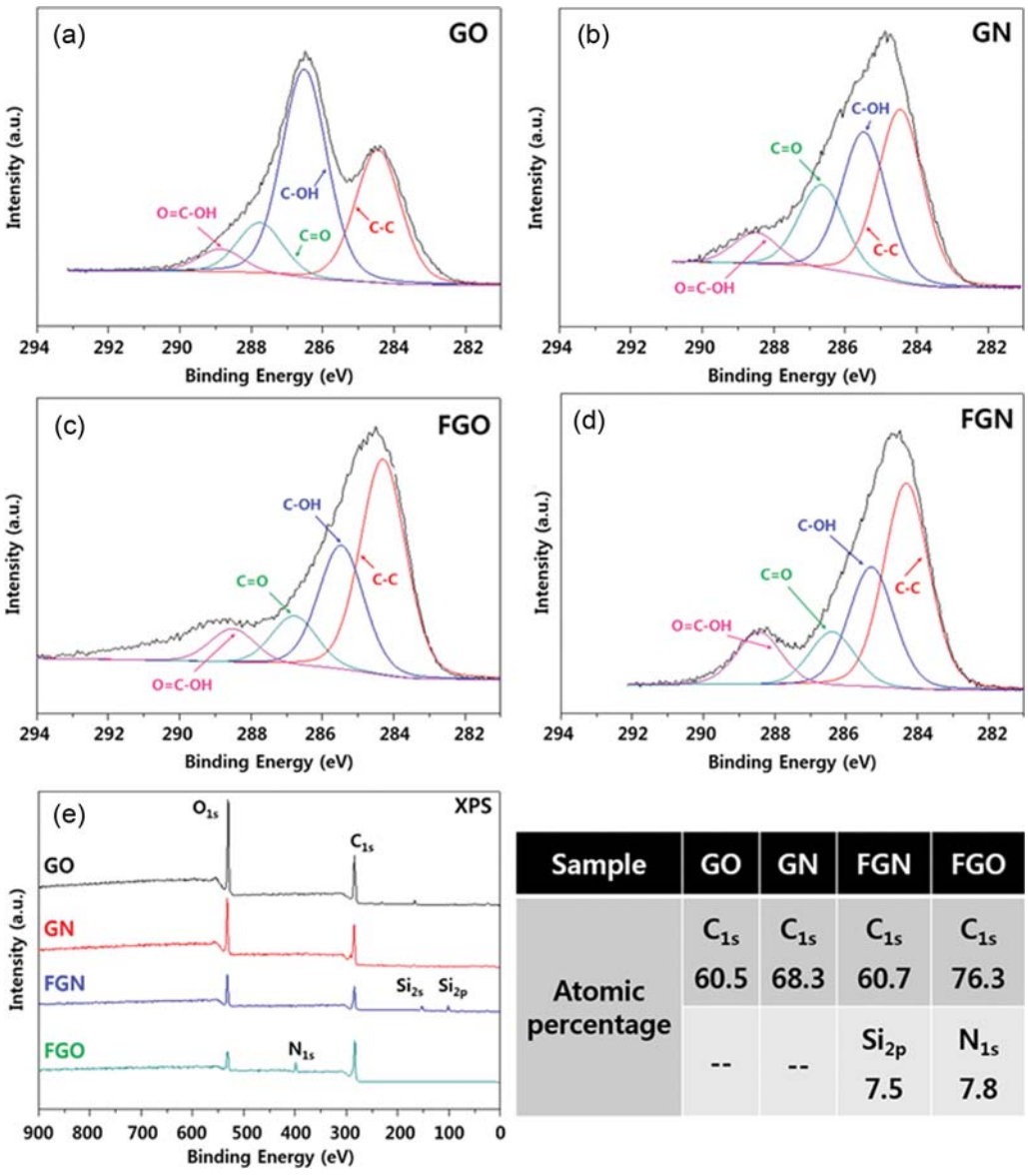

Sample	GO	GN	FGN	FGO
Atomic percentage	C_{1s} 60.5	C_{1s} 68.3	C_{1s} 60.7	C_{1s} 76.3
	--	--	Si_{2p} 7.5	N_{1s} 7.8

Fig. 3. C_{1s} magnified of XPS spectra of (a) GO, (b) GN, (c) FGO, (d) FGN, and (e) XPS analysis of GO, GN, FGO, and FGN.

Table 1. Gel content of AESO and nano-composite films

Filler content (%)	Gel content (%)			
	AESO/GO	AESO/FGO	AESO/GN	AESO/FGN
0	97.15	97.15	97.15	97.15
0.02	99.58	98.98	98.25	99.12
0.05	98.15	97.85	97.36	98.15
0.10	98.69	98.58	97.98	98.56
0.15	96.98	98.05	98.15	98.15
0.20	97.95	98.58	-	-
0.25	99.18	98.36	-	-

(Fig. 4). It is observed that the incorporation of 0.05% GO leads to ~10% increase in tensile strength of AESO composite and there is no increment with addition of further GO content (Fig. 4(a)). Whereas, the addition of 0.02% FGO leads to the same amount of increment in tensile strength, and the increment is observed till ~30% after addition of 0.20% FGO (Fig. 4(b)). In case of AESO/GN and AESO/FGN composites, the incorporation of 0.02% FGN leads to a ~48% increase in tensile strength (Fig. 4(d)). However, at the same loading of GN (Fig. 4(c)), AESO composite only displays ~8% increase, and the incorporation of 0.10% GN leads to ~30% increase. Without functionalization of fillers, the composite fabricated using GN shows higher tensile strength than GO composite. Similarly, after functionalization, FGN composite exhibits higher improvement in the tensile strength than FGO. From the above data, it can be concluded that the functionalization of GO and GN significantly improves the dispersion of the fillers, which results in higher tensile strength even with lower content of fillers. Grafting of organic molecules with GO or GN inhibits the stacking and agglomeration of the GO or GN sheets and helps to improve dispersion.

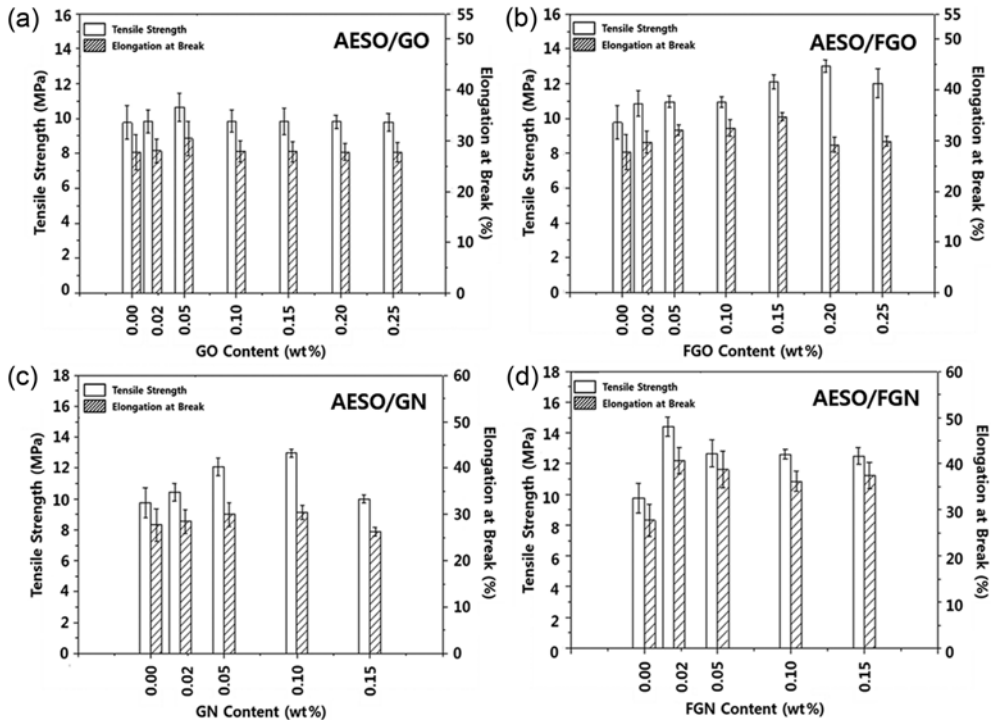

Fig. 4. The tensile strength and elongation at break of (a) AESO/GO, (b) AESO/FGO, (c) AESO/GN, and (d) AESO/FGN composite films.

Table 2. Data for one-way analysis of variance (ANOVA) for comparison of mechanical properties

Mechanical properties	Sample name	Source of variation	SS	DF	MS	F	P value	P critical
Tensile strength	GO	Between groups	2.031	6	0.338	0.738	0.627	2.847
		Within groups	6.42	14	0.458			
		Total	8.451	20				
	FGO	Between groups	21.860	6	3.643	11.145	0.000	2.847
		Within groups	4.576	14	0.326			
		Total	26.436	20				
	GN	Between groups	23.699	4	5.924	17.800	0.000	3.478
		Within groups	3.328	10	0.332			
		Total	27.028	14				
	FGN	Between groups	33.144	4	8.286	16.831	0.000	3.478
		Within groups	4.922	10	0.492			
		Total	38.067	14				
% Elongation	GO	Between groups	18.349	6	3.058	0.515	0.789	2.847
		Within groups	83	14	5.928			
		Total	101.349	20				
	FGO	Between groups	101.329	6	16.888	5.254	0.005	2.847
		Within groups	44.993	14	3.213			
		Total	146.322	20				
	GN	Between groups	33.496	4	8.374	1.560	0.258	3.478
		Within groups	53.660	10	5.366			
		Total	87.156	14				
	FGN	Between groups	295.907	4	73.976	7.578	0.004	3.478
		Within groups	97.613	10	9.761			
		Total	393.520	14				

SS: Sum of squares, DF: Degree of freedom, MS: Mean square

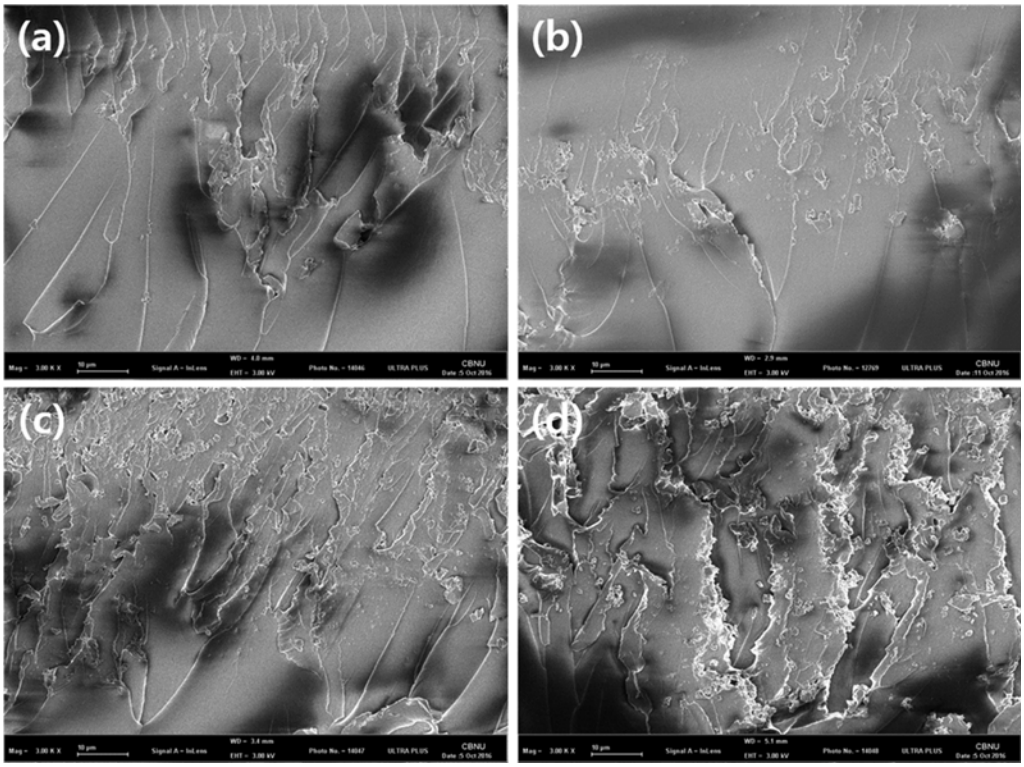

Fig. 5. FE-SEM micrographs of fractured surface of (a) AESO/GO, (b) AESO/GN, (c) AESO/FGO, and (d) AESO/FGN composite films (Scale bar: 10 μm).

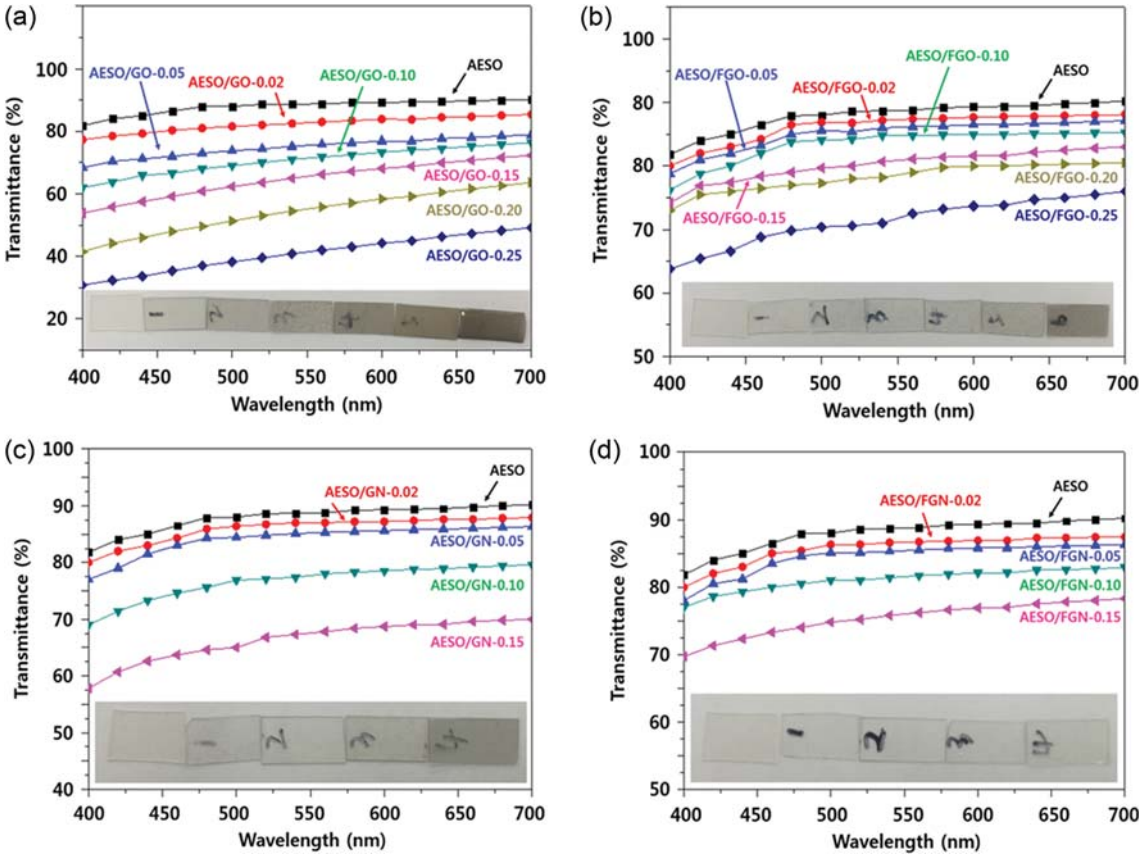

Fig. 6. UV-Vis spectra of (a) AESO/GO, (b) AESO/FGO, (c) AESO/GN, and (d) AESO/FGN composite films.

The chemical bond formation between functionalized groups with acrylate groups after UV curing leads to the formation of network and contributes to the interfacial interaction resulting in higher strength. For comparison of mechanical properties, data for one-way analysis of variance (ANOVA) is shown in Table 2.

To understand the propagation of fracture in tensile direction, the fractured surface of the composite films was observed by electron microscope and presented in Fig. 5. The analysis shows that the AESO composites with GO and GN have fairly smooth surface and the fractures may have propagated in a planar manner. Whereas, the AESO composites with FGO and FGN show significantly uneven surfaces, suggesting that the fractures may have been distorted by FGO or FGN sheets and crack propagation would have been difficult, which may lead to the enhancement in tensile strength.

3. Optical Property

Optical property, i.e., transmittance against wavelength of prepared composites compared to AESO under UV-Vis light, is presented in Fig. 6 along with the digital pictures of the same. A general trend can be seen from the figure that AESO film displays higher transmittance in the visible light region and it is reduced with increased filler content. This reduction can be due to the shielding effect of filler [47]. However, it is also observed that the reduction of transmittance is less for AESO with FGO (from 80 to 64% at 400 nm) in comparison to AESO with GO (from 80 to 31% at 400 nm). Functionalization leads to the homogeneous dispersion of filler into polymer matrix, which results in improved optical property even with higher filler content. Similar effects are observed in case of AESO with GN (from 80 to 58% at 400 nm) and FGN (from 80 to 69% at 400 nm), suggesting that the fillers are homogeneously dispersed in the polymer matrix. The physical inspection of the prepared composite films (shown as inset in the Fig. 6) supports the same effect.

CONCLUSION

We have functionalized graphene and graphene oxide toward a homogeneous dispersion in AESO and formed polymer networks using UV curing technique. The spectroscopic analysis confirms the functionalization of graphene and graphene oxide. Homogeneous dispersion of FGO and FGN leads to an enhancement in the tensile strength of polymer by maximum ~48% even at very low concentration (0.02% FGN content), as compared to that without functionalized graphene composite. Electron microscopic analysis showed fractured surface, and the diverse direction of fracture confirmed the characteristic of toughening factor. The incorporation of functionalized graphene and graphene oxide reduced the transmittance of the composite films; however, it was lower than the non-functionalized fillers composite. Overall, the functionalization of graphene and graphene oxide and their incorporation into the polymer network using UV curing technique provides a realistic and effective methodology to obtain high performance composite for several applications.

ACKNOWLEDGEMENTS

This research was also supported by the National Research Foundation of Korea (NRF-2017R1A2B4002371).

REFERENCES

1. S. S. Sawant, B. K. Salunke, T. K. Tran and B. S. Kim, *Korean J. Chem. Eng.*, **33**, 1505 (2016).
2. P. Saithai, V. Tanrattanakul, W. Chinpa, K. Kaewtathip and E. Dubreucq, *Mater. Sci. Forum*, **695**, 320 (2011).
3. T. Varaporn and S. Pimchanok, *J. Appl. Polym. Sci.*, **114**, 3057 (2009).
4. H. M. Kim, H. R. Kim and B. S. Kim, *J. Polym. Environ.*, **18**, 291 (2010).
5. N. R. Jang, H. R. Kim, C. T. Hou and B. S. Kim, *Polym. Adv. Technol.*, **24**, 814 (2013).
6. R. Auvergne, S. Caillol, G. David, B. Boutevin and J.-P. Pascault, *Chem. Rev.*, **114**, 1082 (2014).
7. I. Tarnavchyk, A. Popadyuk, N. Popadyuk and A. Voronov, *ACS Sust. Chem. Eng.*, **3**, 1618 (2015).
8. M. A. Mosiewicki and M. I. Aranguren, *Eur. Polym. J.*, **49**, 1243 (2013).
9. M. L. Robertson, K. Chang, W. M. Gramlich and M. A. Hillmyer, *Macromolecules*, **43**, 1807 (2010).
10. D. Åkesson, M. Skrifvars and P. Walkenström, *J. Appl. Polym. Sci.*, **114**, 2502 (2009).
11. W. Thielemans, E. Can, S. S. Morye and R. P. Wool, *J. Appl. Polym. Sci.*, **83**, 323 (2002).
12. B. Dong, Y. Yuan, J, Luo, L, Dong, R. Liu and X. Liu, *Prog. Org. Coat.*, **118**, 57 (2018).
13. Q. Zhang, J. Wang, J. Yu and Z.-X. Guo, *Soft Matter*, **13**, 3431 (2017).
14. W. Thielemans, I. M. McAninch, V. Barron, W. J. Blau and R. P. Wool, *J. Appl. Polym. Sci.*, **98**, 1325 (2005).
15. W. Liu, M. Fei, Y. Ban, A. Jia and R. Qiu, *Polymers*, **9**, 541 (2017).
16. C. Lee, X. Wei, J. W. Kysar and J. Hone, *Science*, **321**, 385 (2008).
17. F. Abbasi, J. Karimi-Sabet, C. Ghotbi and Z. Abbasi, *Korean J. Chem. Eng.*, **35**, 1174 (2018).
18. G. Lee and B. S. Kim, *Biotechnol. Prog.*, **30**, 463 (2014).
19. C. Dongyu, Y. Kamal and S. Mo, *Nanotechnology*, **20**, 085712 (2009).
20. J. R. Potts, S. H. Lee, T. M. Alam, J. An, M. D. Stoller, R. D. Piner and R. S. Ruoff, *Carbon*, **49**, 2615 (2011).
21. H. Ha and C. J. Ellison, *Korean J. Chem. Eng.*, **35**, 303 (2018).
22. G. Gonçalves, P. A. A. P. Marques, A. Barros-Timmons, I. Bdkin, M. K. Singh, N. Emami and J. Grácio, *J. Mater. Chem.*, **20**, 9927 (2010).
23. C. Rodríguez-González, A. L. Martínez-Hernández, V. M. Castaño, O. V. Kharissova, R. S. Ruoff and C. Velasco-Santos, *Ind. Eng. Chem. Res.*, **51**, 3619 (2012).
24. X. Wang, Y. Hu, L. Song, H. Yang, W. Xing and H. Lu, *J. Mater. Chem.*, **21**, 4222 (2011).
25. A. Liang, X. Jiang, X. Hong, Y. Jiang, Z. Shao and D. Zhu, *Coatings*, **8**, 33 (2018).
26. D. W. Johnson, B. P. Dobson and K. S. Coleman, *Curr. Opin. Colloid Interf. Sci.*, **20**, 367 (2015).
27. Y. J. Noh, H.-I. Joh, J. Yu, S. H. Hwang, S. Lee, C. H. Lee, S. Y. Kim and J. R. Youn, *Sci. Rep.*, **5**, 9141 (2015).
28. Y. Fu, L. Liu and J. Zhang, *ACS Appl. Mater. Inter.*, **6**, 14069 (2014).
29. J. Cho, I. Jeon, S. Y. Kim, S. Lim and J. Y. Jho, *ACS Appl. Mater.*

Inter., **9**, 27984 (2017).
30. L. Dong, Z. Chen, X. Zhao, J. Ma, S. Lin, M. Li, Y. Bao, L. Chu, K. Leng, H. Lu and K. P. Loh, *Nat. Commn.*, **9**, 76 (2018).
31. M. J. Allen, V. C. Tung and R. B. Kaner, *Chem. Rev.*, **110**, 132 (2010).
32. M. Fang, K. Wang, H. Lu, Y. Yang and S. Nutt, *J. Mater. Chem.*, **19**, 7098 (2009).
33. M. C. Hsiao, S. H. Liao, Y. F. Lin, C. A. Wang, N. W. Pu, H. M. Tsai and C. C. Ma, *Nanoscale*, **3**, 1516 (2011).
34. S. Jianfeng, H. Yizhe, L. Chen, Q. Chen and Y. Mingxin, *Small*, **5**, 82 (2009).
35. H. Kim, Y. Miura and C. W. Macosko, *Chem. Mater.*, **22**, 3441 (2010).
36. Y. Xu, Z. Liu, X. Zhang, Y. Wang, J. Tian, Y. Huang, Y. Ma, X. Zhang and Y. Chen, *Adv. Mater.*, **21**, 1275 (2009).
37. L. M. Veca, F. Lu, M. J. Meziani, L. Cao, P. Zhang, G. Qi, L. Qu, M. Shrestha and Y.-P. Sun, *Chem. Commun.*, **18**, 2565 (2009).
38. Z. Liu, J. T. Robinson, X. Sun and H. Dai, *J. Am. Chem. Soc.*, **130**, 10876 (2008).
39. X. Wang, W. Xing, L. Song, B. Yu, Y. Hu and G. H. Yeoh, *React. Funct. Polym.*, **73**, 854 (2013).
40. B. Yu, X. Wang, W. Xing, H. Yang, L. Song and Y. Hu, *Ind. Eng. Chem. Res.*, **51**, 14629 (2012).
41. J. Wen, B. K. Salunke and B. S. Kim, *J. Chem. Technol. Biot.*, **92**, 1428 (2017).
42. B. K. Salunke and B. S. Kim, *RSC Adv.*, **6**, 17158 (2016).
43. X. Li, G. Zhang, X. Bai, X. Sun, X. Wang, E. Wang and H. Dai, *Nat. Nanotechnol.*, **3**, 538 (2008).
44. S. C. Mauck, S. Wang, W. Ding, B. J. Rohde, C. K. Fortune, G. Yang, S.-K. Ahn and M. L. Robertson, *Macromolecules*, **49**, 1605 (2016).
45. M.-C. Hsiao, S.-H. Liao, M.-Y. Yen, P.-I. Liu, N.-W. Pu, C.-A. Wang and C.-C. M. Ma, *ACS Appl. Mater. Inter.*, **2**, 3092 (2010).
46. X. Fan, W. Peng, Y. Li, X. Li, S. Wang, G. Zhang and F. Zhang, *Adv. Mater.*, **20**, 4490 (2008).
47. M. Martin-Gallego, R. Verdejo, M. A. Lopez-Manchado and M. Sangermano, *Polymer*, **52**, 4664 (2011).